Available online at www.sciencedirect.com
SCIENCE DIRECT®
ELSEVIER
Marine Structures 17 (2004) 91–123
MARINE STRUCTURES
www.elsevier.com/locate/marstruc

Maintained ship hull xcgirxcder ultimate strength reliability considering corrosion and fatigue

Yong Hu[a,b], Weicheng Cui[a,*], Preben Terndrup Pedersen[c]

[a]*School of Naval Architecture and Ocean Engineering, Shanghai Jiao Tong University, Shanghai, 200030, China*
[b]*Wuhan Second Ship Design and Research Institute, Wuhan, P.O.Box 64196, 430064, China*
[c]*Department of Mechanical Engineering, Technical University of Denmark, Building 101E, DK 2800 Lyngby, Denmark*

Received 23 October 2003; received in revised form 26 April 2004; accepted 4 June 2004

Abstract

The purpose of this paper is to propose a methodology to assess the time-variant ultimate strength of ship hull girder under the degradations of corrosion and fatigue. The effects of fatigue cracks on the tensile and compressive residual ultimate strength of stiffened panels and unstiffened plates are analyzed by an FE method. Based on FE analysis results, some empirical formulae are provided for effective calculation of the compressive or tensile ultimate strength of cracked or intact unstiffened plates or stiffened panels. A non-linear corrosion model is used to determine the corrosion rate of plates, webs and flanges, respectively. The effects of inspection and repair are taken into account. A minimum net thickness rule is used to determine repair policies. A procedure is proposed to determine the maximum allowable corrosion thicknesses of different parts of the hull cross section. The procedure developed is illustrated by application to a tanker. For a given set of inspection and repair criteria, the ultimate bending moment and reliability as a function of ship age is predicted.

Keywords: Hull girder ultimate strength; Corrosion; Fatigue; Repair

*Corresponding author. Tel.: +86-21-6293-2081; fax: +86-21-6293-3160.
E-mail address: wccui@sjtu.edu.cn (W. Cui).

0951-8339/$ - see front matter © 2004 Elsevier Ltd All rights reserved.
doi:10.1016/j.marstruc.2004.06.001

1. Introduction

The International Maritime Organization (IMO), classification societies and ship owners continue to seek acceptable standards for structural integrity of aging ships without excessive economic penalties with respect to repair and maintenance costs incurred over the ship life cycle.

The ultimate strength of ship hull girders will be slowly reduced due to the degradation effects of corrosion and fatigue cracks. On the other hand, the ship hull girder strength can be improved by repair. Therefore ship hull girder strength is an alternately changing process between degradation and rapid improvement in its whole lifetime.

Assessing the residual strength of a ship structure, it has been common to consider three main strength components, which are longitudinal strength, transverse strength and local strength. Among these strengths, longitudinal strength, that is hull girder strength, is the most fundamental and important strength to ensure the safety of a ship structure. With the increase of the applied longitudinal bending moment, the structural members composing a hull cross section begin to collapse one by one due to buckling and yielding.

Usually, three types of limit state modes of a ship hull girder bending moment are used in reliability analysis of ship structures, namely initial yield bending moment, fully plastic bending moment and ultimate bending moment [1].

In Refs. [2–5], an advanced time-variant formulation for the reliability of a ship hull was developed by taking into account the degradation effects of crack growth and corrosion and the improvement effect of repair operations. The first yield reliability of the midship section modulus was analyzed; the limit state for global hull girder failure was defined as initial yield bending moment. In Refs. [6,7], the ship hull girder ultimate strength reliability was analyzed under the degradation effect of corrosion. But the unsteady propagation of fatigue cracks may induce rapid reduction of residual ultimate strength of ship structures. And the unsteady period of crack propagation is very short compared to the inspection interval. The degradation effect of fatigue cracks on the ultimate strength of ship hull girder still needs further investigation.

The ultimate bending moment of the ship hull girder is associated with the compressive and tensile ultimate strength of stiffened panels between bulkheads or web frames and unstiffened plates between stiffeners. There are some simplified analytical methods and empirical formulae that can be used to calculate the compressive ultimate strength of stiffened panels and unstiffened plates for intact structures [8,9]. But for aging ships, the fatigue cracks and corrosion will degrade the ultimate strength of stiffened panels and unstiffened plates. The residual ultimate strength of unstiffened plates and stiffened panels with corrosion and crack damage should be assessed properly. And the damage degree of corrosion and fatigue cracks should be determined at first to assess the strength of aging ships.

Usually, general corrosion modes are used to calculate the corrosion damage and the structural strength can be analyzed by intact structural methods with a

degradation of geometric dimensions [3–7,10]. Constant corrosion model is usually used to assess the wastage of corrosion. But now, more and more researches indicate that non-linear corrosion models are more reasonable [11,12]. To consider the effect of fatigue cracks on the structure's residual ultimate strength, there are still very few comprehensive studies presented. The most ordinary method to deal with such condition is simply subtracting the crack area from the total member's area. This simplified method will overestimate the ultimate strength.

In this study, a methodology for the time-variant reliability assessment relative to the ultimate strength of ship hull girder with the degradation of corrosion and fatigue is presented. The effect of fatigue crack on the tensile and compressive residual ultimate strength of stiffened panels and unstiffened plates are analyzed by an FE method. Based on FE analysis results, some empirical formulae are obtained to calculate the compressive or tensile ultimate strength of cracked or intact unstiffened plates or stiffened panels. A non-linear corrosion model is used to calculate the corrosion rate of plate, web and flange, respectively. The Caldwell's method is applied to calculate the residual ultimate bending moment of aging ship hull girder. Three types of limit states of aging ship hull girders are compared. The effects of inspection and repair are taken into account. A minimum net thickness rule is used to determine repair policies. The procedure developed is illustrated by application to a tanker. For a given set of inspection and repair criteria, ultimate bending moment and reliability as a function of ship age is predicted.

2. The residual ultimate strength of unstiffened plates and stiffened panels with fatigue crack damage

The residual ultimate tensile and compressive strength of a plate with different crack length a can be calculated by two methods. One is the FE method; the other is a simplified method (assuming that the plate is intact and the breadth of the plate is $B-a$). Fig. 1 shows an unstiffened plate with a center crack subjected to longitudinal

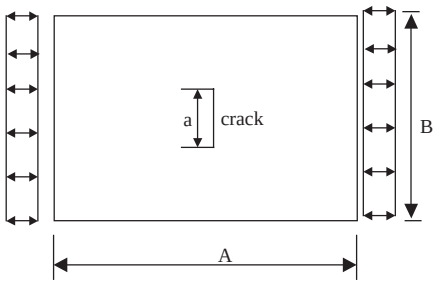

Fig. 1. An initially cracked plate subjected to longitudinal uniform loads.

uniform loads. The geometric and material properties of the plate are assumed as follows:

Length $A = 1000\,\text{mm}$; breadth $B = 1000\,\text{mm}$; thickness $t = 10\,\text{mm}$; Young's modulus $E = 2.1 \times 10^5\,\text{N/mm}^2$; Poisson ratio $v = 0.3$; yield stress $\sigma_y = 300\,\text{MPa}$; ultimate tensile stress $\sigma_T = 390\,\text{MPa}$; strain-hardening coefficient $H = 0.003\,\text{E}$.

Fig. 2a shows the residual ultimate strength with different crack lengths obtained by above simplified method and FEM. For simplified method in Fig. 2a, one takes the ultimate tensile stress σ_T as the tensile ultimate strength of intact plate. Fig. 2b shows the relative errors of the two methods.

From Fig. 2 one can find that fatigue crack influences the unstiffened plates residual ultimate strength of the unstiffened plates obviously when the unstiffened plates are subjected to tensile stress. And there is an obvious difference between the FE results and the results of simplified method. The residual ultimate strength is much larger by the simplified method than by FEM. But when the plate is subjected to compressive stress, the effect of a crack on the compressive ultimate strength is not obvious especially when the crack is small. And the difference between FE results and the results of simplified method is not apparent.

Fig. 2a indicates that the most important influence of a crack on the residual ultimate strength of unstiffened plates and stiffened panels is the tensile residual ultimate strength. Many factors such as material parameters (Young's modulus E, initial yield strength σ_Y, ultimate tensile strength σ_T, critical rupture strain ε_R), crack geometries, critical stress intensity factor K_C, will affect the residual ultimate strength of unstiffened plates and stiffened panels. When the intensity factor of crack tips exceeds critical stress intensity factor K_C, the crack will propagate. And the tensile strength reaches the ultimate tensile strength at this moment.

When a crack propagates, the strains at the areas near the crack tips are slightly greater than the material rupture strain ε_R. Because one pays more attention to the whole mechanical capability of structural elements rather than that of the crack tip, the material rapture strain ε_R can be used as crack propagation criterion. And then, the material parameters are simplified. Ordinary elastic-plastic FE method can be applied to calculate the residual ultimate strength of the structural elements with refined meshes around the crack tips. The material stress–strain curve can be simplified as shown in Fig. 3. Because the crack propagation criterion is based on the material rapture strain instead of critical stress intensity factor K_C and the stress–strain curve is idealized as shown in Fig. 3, it is this simplified FE method to calculate the residual ultimate strength of the cracked plate.

By using this simplified FE method, the results are reliable with errors under 3% compared to test results [10], see Table 1.

In order to simplify the calculation procedure, the following empirical formulae can be used to calculate the residual ultimate strength of unstiffened plates and stiffened panels with center crack or edge crack damage. These formulae are obtained based on simplified FEM results described above and test results.

When the unstiffened plate is subjected to tensile stress, the material yield strength σ_Y and nominal crack length (a/B) are the most important factors that determine the residual ultimate tensile strength of the cracked unstiffened plate. Here a plate as shown in Fig. 1 is used. The nominal crack length varies from 0 to 0.9. According to

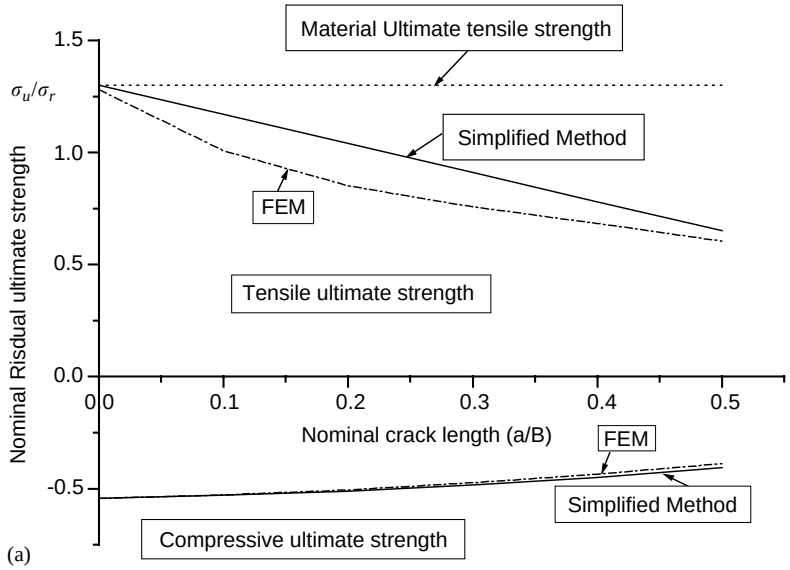

(a)

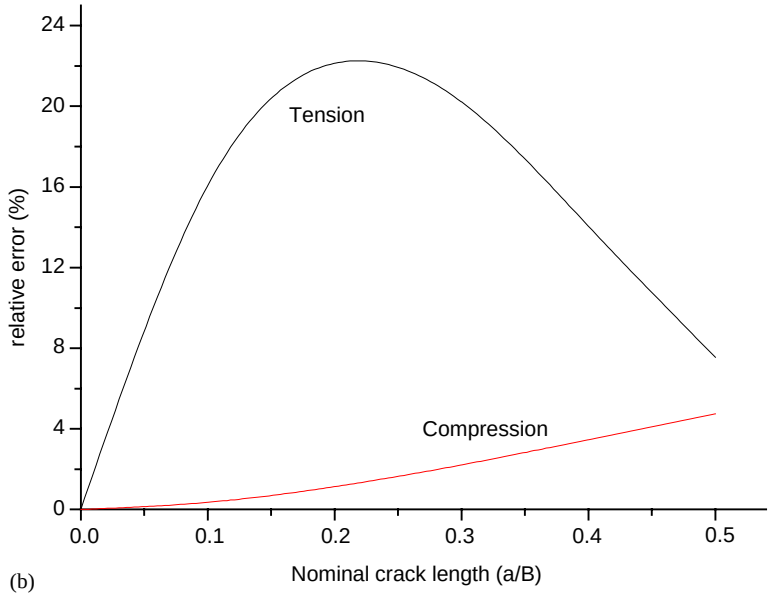

(b)

Fig. 2. a. Residual ultimate strength of a cracked plate under axial tension and compression loads obtained by FEM and simplified method. b. Relative errors between FEM and simplified method.

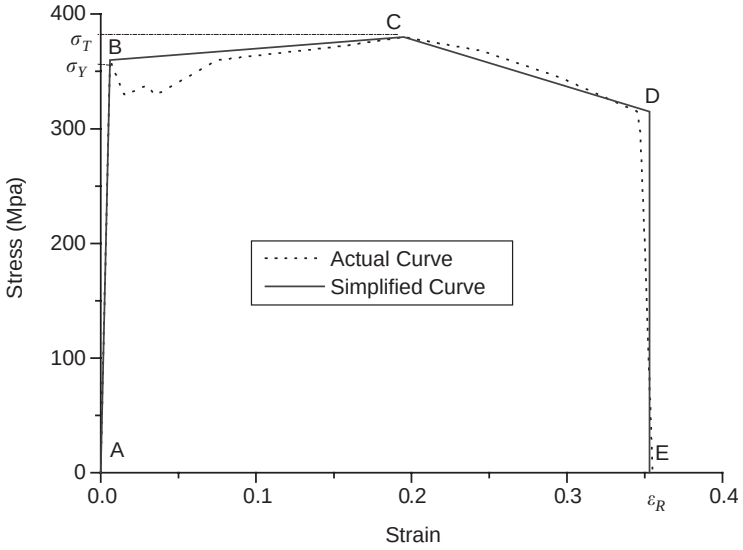

Fig. 3. Simplified strain–stress curve.

Table 1
Comparisons of simplified FEM with test results

Test sample No.	Crack type	Crack length (a/B)	Result (σ_u/σ_Y)		
			FEM	Test [10]	Relative error (%)
1	center	0.03	1.00507	0.98605	1.9
2	center	0.06	0.98244	0.954	2.97
3	center	0.12	0.93347	0.91209	2.34
4	edge	0.03	1.03684	1.01962	1.69
5	edge	0.06	1.00681	1.0012	0.56
6	edge	0.12	0.9509	0.97117	−2.0
7	edge	0.06	0.9915	0.9858	0.59

the FE results, the empirical formulae can be obtained

$$\phi_{cux}(t) = \sigma_u(t)/\sigma_Y = 1.279 - 3.50[a(t)/B] + 8.974[a(t)/B]^2 - 11.975[a(t)/B]^3 + 5.231\left[a(t)/B\right]^4. \quad \text{for center crack,} \tag{1}$$

$$\phi_{eux}(t) = \sigma_u(t)/\sigma_Y = 1.281 - 4.045[a(t)/B] + 6.616[a(t)/B]^2 - 5.194[a(t)/B]^3 + 1.355[a(t)/B]^4 \quad \text{for edge crack,} \tag{2}$$

where σ_Y is the material yield stress, $a(t)$ is the crack length at given time t, B is the plate width, $\phi_{cux}(t)$ and $\phi_{cux}(t)$ are the nominal ultimate strength of plate under tensile load at given time t with center crack and edge crack, respectively.

The variance of $\phi_{cux}(t)$ and $\phi_{cux}(t)$ are determined by the following equations:

$$D_{\phi_{eux}(t)} = \{-3.497/B + 17.948 \cdot [\overline{a(t)}/B^2] - 35.924 \cdot [\overline{a(t)}^2/B^3] + 20.921 \cdot [\overline{a(t)}^3/B^4]\}^2 \cdot D_{a(t)}, \tag{3}$$

$$D_{\phi_{eux}(t)} = \{-4.045/B + 13.232 \cdot [\overline{a(t)}/B^2] - 15.582 \cdot [\overline{a(t)}^2/B^3] + 5.418 \cdot [\overline{a(t)}^3/B^4]\}^2 \cdot D_{a(t)}, \tag{4}$$

where $\mathrm{D}_{\phi_{eux}(t)}, \mathrm{D}_{\phi_{eux}(t)}$ and $D_{a(t)}$ are the variance of $\phi_{cux}(t)$, $\phi_{eux}(t)$ and a(t), respectively, $\overline{a(t)}$ is the mean value of crack length a at given time t.

In the following, we denote $\overline{\mathrm{X}}$ as the mean value of X and D_X as its variance.

When the unstiffened plate is subjected to compressive stress, the material yield strength σ_Y, nominal crack length (a/B) and the slenderness of the plate are the most important factors that determine the residual ultimate compressive strength of the cracked unstiffened plate. Here a plate with a length of $A = 2400$ mm, a breadth of $B = 800$ mm is used. The slenderness of the plate varies from 1 to 5. The nominal crack length varies from 0 to 0.9. According to the FE results, the empirical formula of the ultimate strength of the cracked plate can be expressed as

$$\phi_{u-x}(t) = 0.104287 + \phi_\beta(t) \cdot \phi_{C/B}(t), \tag{5}$$

where $\phi_{u-x}(t) = \sigma_{u-x}(t)/\sigma_Y$ is the nominal ultimate strength of the cracked plate under compressive load, $T(t)$ is the thickness of the plate at given time t and

$$\phi_\beta(t) = 1.31071 - 0.35075 \cdot \beta(t) + 0.03006\beta \cdot (t)^2 - 0.0000277779 \cdot \beta(t)^3,$$

$$\phi_{C/B}(t) = 0.830528 - 0.23082 \cdot [a(t)/B] - 0.67362 \cdot [a(t)/B]^2 - 0.0829 \cdot [a(t)/B]^3,$$

$$\beta(t) = \frac{B}{T(t)} \sqrt{\frac{\sigma_Y}{E}}.$$

The variance of $\phi_{u-x}(t)$ can be calculated as follows:

$$D_{\phi_{u-x}(t)} = \overline{\phi_\beta(t)}^2 D_{\phi_{C/B}(t)} + \overline{\phi_{C/B}(t)}^2 D_{\phi_\beta(t)}, \tag{6}$$

where

$$D_{\beta(t)} = \left[\frac{B}{\overline{T(t)}^2}\sqrt{\frac{\overline{\sigma_Y}}{\overline{E}}}\right]^2 \cdot D_{T(t)} + \left[\frac{B}{2.\overline{T(t)}}\sqrt{\frac{1}{\overline{\sigma}_Y.\overline{E}}}\right]^2 \cdot D_{\sigma_Y} + \left[\frac{B.\overline{E}}{2.\overline{T(t)}}\sqrt{\frac{\overline{\sigma_Y}}{E}}\right]^2 \cdot D_E,$$

$$D_{\phi_\beta(t)} = [-0.35075 + 0.06012 \cdot \overline{\beta(t)} - 0.00008333379 \cdot \overline{\beta(t)}^2]^2 \cdot D_{\beta(t)},$$

$$D_{\phi_{C/B}(t)} = [-0.23082/B - 1.3472 \cdot \overline{a(t)}/B^2 - 0.2487 \cdot \overline{a(t)}^2/B^3]^2 \cdot D_{a(t)}.$$

When a stiffened panel is subjected to tensile stress, see Fig. 4, the web has an edge crack damage and the plating has a center crack damage, the equivalent tensile residual ultimate strength is

$$\sigma_{usp}(t) = \phi_{us}(t) \cdot \sigma_{Ys} \cdot t_w(t) \cdot h_w + \phi_{up}(t) \cdot \sigma_{Yp} \cdot t_p(t) \cdot b, \tag{7}$$

where $\sigma_{usp}(t)$ is the ultimate strength of the stiffened panel under tensile load, σ_{Ys} is the stiffener's yield stress,σ_{Yp} is the plate's yield stress, $\phi_{up}(t)$ can be obtained through Eq. (1), $\phi_{us}(t)$ can be obtained through Eq. (2). The variance of $\sigma_{usp(t)}$ can be calculated as follows:

$$\begin{aligned} D_{\sigma_{usp}}(t) = {} & \left[\overline{\sigma_{Ys}} \cdot \overline{t_w(t)} \cdot h_w\right]^2 \cdot D_{\phi_{uS}(t)} + \left[\overline{\phi_{us}(t)} \cdot \overline{t_w(t)} \cdot h_w\right]^2 \cdot D_{\sigma_{Ys}} \\ & + \left[\overline{\phi_{us}(t)} \cdot \overline{\sigma_{Ys}} \cdot h_w\right] \cdot D_{t_w(t)} \\ & + \left[\overline{\sigma_{Yp}} \cdot \overline{t_p(t)} \cdot b\right]^2 \cdot D_{\phi_{up}(t)} + \left[\overline{\phi_{up}(t)} \cdot \overline{t_p(t)} \cdot hb\right]^2 \cdot D_{\sigma_{Yp}} \\ & + \left[\overline{\phi_{up}(t)} \cdot \overline{\sigma_{Yp}} \cdot b\right] \cdot D_{t_p(t)}. \end{aligned} \tag{8}$$

When the stiffened panels and unstiffened plates are intact structures, Eqs. (1), (2) and (5) can also be used to assess the ultimate strength. Some simplified methods,

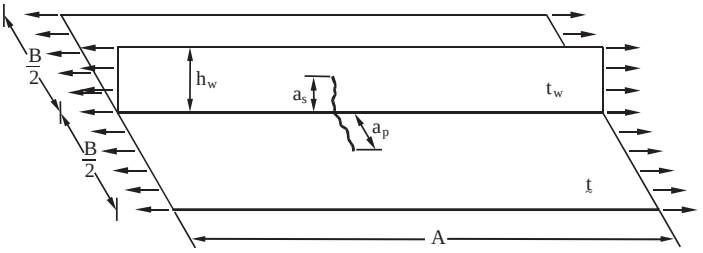

Fig. 4. An initially cracked stiffened plate.

such as elastic–plastic simplified analytical method [8,9], can be used to predict the compressive ultimate strength of the intact plate.

3. Crack propagation prediction

To predict the crack propagation and fatigue life, the Paris–Erdogan equation is used

$$\frac{\mathrm{d}a(t)}{\mathrm{d}N} = C\Delta K^m, \tag{9}$$

where $a(t)$ is the crack length at given time t, N is the number of cycles, ΔK is the stress intensity factor range and C and m are material parameters. The stress intensity factor range is given by

$$\Delta K = \Delta\sigma Y(a)\sqrt{\pi a}, \tag{10}$$

where $\Delta\sigma$ is the stress range and $Y(a)$ is the geometry function. If $Y(a) = Y$ is a constant and $N = v_0 t$ where v_0 is the mean zero uncrossing rate and t is the time, then integration of Eq. (9) gives

$$a(t) = \left[a_0^{1-m/2} + \left(1 - \frac{m}{2}\right) C\Delta\sigma^m Y^m \pi^{m/2} v_0 t\right]^{2/(2-m)}, \quad m \neq 2, \tag{11}$$

$$a(t) = a_0 \exp\left(CY^2\Delta\sigma^2\pi v_0 t\right), \quad m = 2. \tag{12}$$

The complete fatigue life T_f is equal to the sum of the time of crack propagation Tp with the time of crack initiation T_i [3]

$$T_f = T_i + T_p. \tag{13}$$

The probability distribution of the time of crack initiation is approximated by a Weibull distribution [3]:

$$F_{T_i}(t_i) = 1 - \exp\left[-\left(\frac{t_i}{\beta_{T_i}}\right)^{\alpha_{T_i}}\right]. \tag{14}$$

It is practical and sufficiently accurate to assume that the time to crack initiation is related to the time to reach critical size a_{cr} by

$$T_i = kT_p, \tag{15}$$

where k can vary between 0.1 and 0.15 [3].

To calculate the time of crack propagation, the critical crack length a_{cr} should be determined first. When the residual ultimate strength of the unstiffened plate or stiffened panel is lower than the maximum external load, the crack will propagate unstably. The crack length has reached its critical size. So using Eqs. (1), (2) and (5) the critical crack length can be determined for a given external load.

Using Eq. (11) the mean value and variance of the crack propagation length is given by

$$\overline{a(t)} = \left[\overline{a_0}^{1-m/2} + \left(1-\frac{m}{2}\right)\overline{C\Delta\sigma}^{m} Y^m \pi^{m/2} \cdot v_0 t\right]^{2/(2-m)}, \tag{16}$$

$$\begin{aligned} D_{a(t)} = & \left[\frac{\overline{a_0}^{m/2}\overline{a(t)}}{\overline{a_0}^{1-m/2} + (1-m/2)\overline{C\Delta\sigma}^{m} Y^m \pi^{m/2} v_0 t}\right]^2 D_{a_0} \\ & + \left[\frac{\overline{\Delta\sigma^m} Y^m \pi^{m/2} v_0 t \overline{a(t)}}{\overline{a_0}^{1-m/2} + (1-m/2)\overline{C\Delta\sigma}^{m} Y^m \pi^{m/2} v_0 t}\right]^2 D_C \\ & + \left[\frac{\overline{C\Delta\sigma}^{m} Y^m \pi^{m/2}}{\overline{a_0}^{1-m/2} + (1-m/2)\overline{C\Delta\sigma}^{m} Y^m \pi^{m/2} v_0 t}\right]^2 D_{a_0}. \end{aligned} \tag{17}$$

4. Corrosion damage model

Corrosion is one of the most important damage types for ship structures. The corrosion rate of ship hull structures is influenced by many factors including the corrosion protection system (e.g. coating and anodes) and various operational parameters such as the percentage of time in ballast, the type of cargo, component location and orientation, level of oxygen, temperature, degree of flexibility, frequency and method of tank cleaning, maintenance and repair.

In most studies, the effect of corrosion is represented by an uncertain but constant corrosion rate, which results in a linear decrease of plate thickness with time. This model may be useful for calculate the wastage of upper-surface of inner bottom plating and low sloping plating. Because those plates surfaces are usually uncoated, abrasion from cargo and impact from unloading gear are the general abrasion forms [11]. For other locations, coating are present, the progress of corrosion would normally depend on the degradation of coating. Therefore, for the coated elements, the corrosion model can be divided into two phases. The first phase is no corrosion occurrence due to coating protection. The second phase is corrosive phase.

To calculate the first phase, the life of coating may be assumed to follow a normal distribution given by [11]

$$f(t) = \frac{1}{\sqrt{2\pi}\sigma} \exp\left(-\frac{(t-\mu)^2}{2\sigma^2}\right), \tag{18}$$

where μ is the mean value of the coating life ; σ is the standard deviation of the coating life. The mean value of the coating life is around 10 years and the coefficient of variation of coating life is about 0.4 for tankers.

After the coating is lost, corrosion will gradually start. Non-linear corrosion model is more appropriate than linear corrosion model in this phase. The corrosion rate will go from accelerative corrosion rate to decelerative rate due to the protection

of the corroded material. A Weibull function is assumed to describe the corrosion rate in this corrosion phase. The corrosion rate can be described by [12]

$$r(t) = \begin{cases} 0, & 0 \leqslant t \leqslant T_{st}, \\ d_\infty \frac{\beta}{\eta} \left(\frac{t-T_{st}}{\eta}\right)^{\beta-1} \exp\left\{-\left(\frac{t-T_{st}}{\eta}\right)^{\beta}\right\}, & T_{st} \leqslant t \leqslant T_L, \end{cases} \tag{19}$$

where $r(t)$ is the corrosion rate, d_∞ is the long-term thickness of the corrosion wastage, T_{st} is the coating life,β and η are Weibull parameters.

Using this corrosion model, the wear of thickness due to corrosion can be calculated by definition,

$$d(t) = \begin{cases} 0, & 0 \leqslant t \leqslant T_{st}, \\ d_\infty \left\{1 - \exp\left[-\left(\frac{t-T_{st}}{\eta}\right)^{\beta}\right]\right\}, & T_{st} \leqslant t \leqslant T_L. \end{cases} \tag{20}$$

In Eq. (20), there are four parameters to be determined. This is a non-linear regression problem. There are two methods to determine these parameters [12]. In the first method, the four parameters are assumed to be deterministic while in the second method the four parameters are assumed to be random. Fig. 5 demonstrates an actual ship bottom plate's corrosion depth measurements at different time and different spots and their fitting function. The measurements are from bulk carriers [11]. The fitted four deterministic parameters are, $T_{st} = 8.24$ years, $\eta = 20.58$, $\beta = 2.81$, $d_\infty = 3.76$ mm. The maximum corrosion rate is achieved at $T_A = 34.34$ years, and its value is $r_{\max} = 0.061$ mm/year.

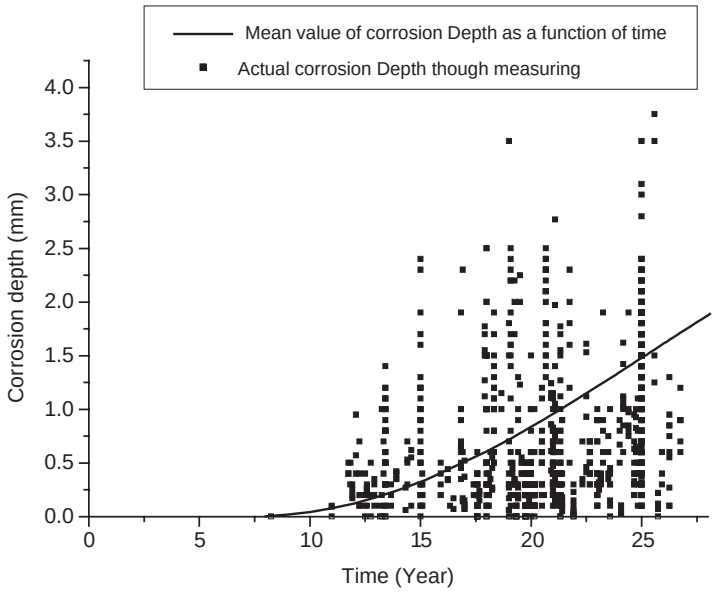

Fig. 5. Actual measured corrosion data [11] and their fitting function.

If all the parameters T_{st}, η, β and d_∞ are assumed to be random variables, the variance of the corrosion rate after corrosion occurs can be calculated as follows:

$$
\begin{aligned}
D_{d_{(t)}} = & \left[1-\exp\left[-\left(\frac{t-\overline{T_{st}}}{\overline{\eta}}\right)^{\overline{\beta}}\right]\right]^2 \cdot D_{d_\infty} \\
& + \left\{\left[\overline{d_\infty}\cdot\exp\left[-\left(\frac{t-\overline{T_{st}}}{\overline{\eta}}\right)^{\overline{\beta}}\right]\right]\cdot\left[\left(\frac{t-\overline{T_{st}}}{\overline{\eta}}\right)^{\overline{\beta}}\cdot In\left(\frac{t-\overline{T_{st}}}{\overline{\eta}}\right)\right]\right\}^2 \cdot D_\beta \\
& + \left[\overline{d_\infty}\cdot\left(\frac{t-\overline{T_{st}}}{\overline{\eta}}\right)^{\overline{\beta}-1}\cdot\frac{\overline{\beta}}{\overline{\eta}}\right]^2 \cdot D_{T_{st}} \\
& + \left[\overline{d_\infty}\cdot\overline{\beta}\cdot\overline{\eta}^{\overline{\beta}-1}\cdot\left(t-\overline{T_{st}}\right)^{\overline{\beta}}\right]^2 \cdot D_\eta. \qquad (21)
\end{aligned}
$$

5. Ship hull's ultimate strength

Vasta [14] assumed that the ship hull would reach the ultimate limit state when the compression flange, i.e. the upper deck in the sagging condition or the bottom plating in the hogging condition, collapses, and that the relationship between the bending moment and curvature is linear. Caldwell [15] took into account buckling in compression and yielding in tension. The ship hull cross section was idealized as an equivalent section with uniform plate thickness in deck, bottom, or sides. When the ship hull reached the ultimate limit state, the entire material in compression was assumed to have reached its ultimate buckling strength and the entire material in compression was assumed to have reached full yielding. However, in the immediate vicinity of the final neutral axis, the side shells will often remain in the elastic state up to the overall collapse of the hull girder. So Paik and Mansour [16] developed Caldwell's method further. They assumed a more credible distribution of longitudinal stresses of the hull cross section at the collapse state, see Fig. 6. Based on this assumption, the formulae for predicting the ultimate strength can be derived.

In Fig. 6, A_B is the total sectional area of outer bottom, A'_B is the total sectional area of inner bottom, A_D is the total sectional area of deck, A_S is the half-sectional area of all sides, D is the hull depth, D_B is the height of double bottom, g is the neutral axis position above the base line in the sagging condition or below the deck in the hogging condition, H is the depth of hull section in linear elastic state, M_{uh} and M_{us} are ultimate bending moment in hogging or sagging conditions, respectively. σ_{yB}, σ_{yB}, σ_{yD}, σ_{ys} are yield strength of outer bottom, inner bottom, deck and side shell, respectively, σ_{uB}, σ_{uB}, σ_{uD}, σ_{us} are ultimate buckling strength of outer bottom, inner bottom, deck and side shell, respectively.

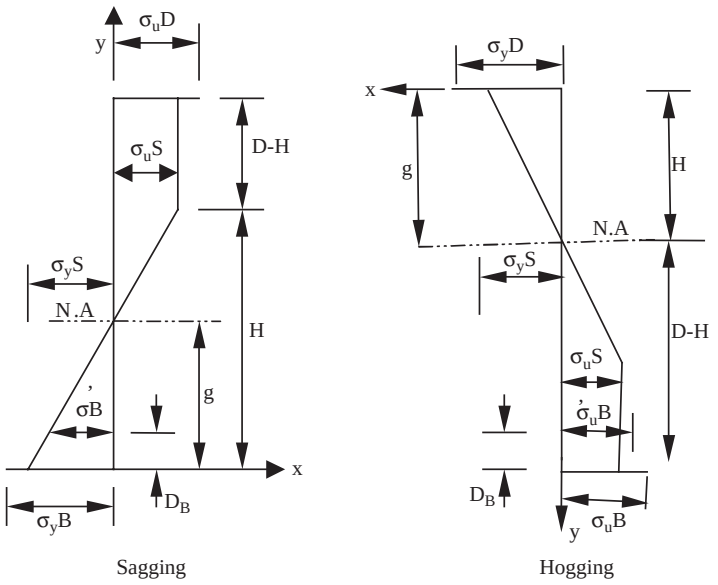

Fig. 6. Assumed distribution of longitudinal stresses in a hull cross section at the overall collapse state.

If the x–y coordinates are taken as shown in Fig. 6, the stress distribution can be expressed by,

In sagging condition

$$\begin{aligned}
\sigma_x(t) &= \sigma_y(t)B \quad \text{at } y = 0 \\
&= -\frac{1}{H(t)}\left[(\sigma_{uS} + \sigma_{yS})y - H(t)\sigma_{yS}(t)\right], \quad 0 < y < H \\
&= \sigma'_B(t) \\
&= -\frac{1}{H(t)}\left\{[\sigma_{uS}(t) + \sigma_{yS}(t)]D_B - H(t)\sigma_{yS}(t)\right\} \quad \text{at } y = D_B \\
&= -\sigma_{uS}(t), \quad H \leqslant y < D \\
&= -\sigma_{uD}(t) \quad \text{at } y = D.
\end{aligned} \tag{22}$$

In hogging condition

$$\begin{aligned}
\sigma_x(t) &= \sigma_y(t)D \quad \text{at } y = 0 \\
&= -\frac{1}{H(t)}\left[(\sigma_{uS}(t) + \sigma_{yS}(t))y - H(t)\sigma_{yS}(t)\right], \quad 0 < y < H \\
&= -\sigma_{uS}(t), \quad H \leqslant y < D \\
&= -\sigma'_{uB}(t) \quad \text{at } y = D - D_B \\
&= -\sigma_{uB}(t) \quad \text{at } y = D.
\end{aligned} \tag{23}$$

From the condition that no axial force acts on the hull girder, the depth of the collapsed sides ($D-H$) can be obtained from.

$$\int \sigma_x(t)\,\mathrm{d}A(t) = 0, \tag{24}$$

$$H(t) = \frac{C_1(t)D + \sqrt{C_1^2(t)D^2 + 4C_2(t)D}}{2}, \tag{25}$$

where

$$C_1(t) = \frac{A_D(t)\sigma_{uD}(t) + 2A_s(t)\sigma_{uS}(t) - A_B(t)\sigma_{yB}(t) - A'_B(t)\sigma_{yS}(t)}{A_S(t)[\sigma_{uS}(t) + \sigma_{yS}(t)]},$$

$$C_2(t) = \frac{A'_B(t)D_B}{A_s(t)}.$$

The position of the neutral axis where the longitudinal stress is zero can be determined by substituting Eqs. (22) and (24) into the following equation

$$g(t) = y|\sigma(t)_{x=0} \tag{26}$$

namely

$$g(t) = \frac{[C_1(t)D + \sqrt{C_1^2(t)D^2 + 4C_2(t)D}]\sigma_{yS}(t)}{2[\sigma_{uS}(t) + \sigma_{yS}(t)]} = H(t)\frac{\sigma_{yS}(t)}{\sigma_{uS}(t) + \sigma_{yS}(t)}. \tag{27}$$

Similarly, in the hogging condition, $g(t)$ and $H(t)$ can be obtained as follows:

$$H(t) = D\frac{A_B(t)\sigma_{uB}(t) + A'_B(t)\sigma'_{uB}(t) + 2A_s(t)\sigma_{uS}(t) - A_D(t)\sigma_{yD}(t)}{A_s(t)[\sigma_{us}(t) + \sigma_{yS}(t)]},$$

$$\begin{aligned} g(t) &= D\,\frac{\begin{array}{c} A_B(t)\sigma_{uB}(t)\sigma_{yS}(t) + A'_B(t)\sigma'_{uB}(t)\sigma_{yS}(t) \\ +2A_s(t)\sigma_{uS}(t)\sigma_{yS}(t) - A_D(t)\sigma_{yD}(t)\sigma_{yS}(t) \end{array}}{A_s(t)[\sigma_{us}(t) + \sigma_{yS}(t)]^2} \\ &= H(t)\,\frac{\sigma_{yS}(t)}{\sigma_{uS}(t) + \sigma_{yS}(t)}. \end{aligned}$$

The ultimate moment capacity of the hull under sagging bending moment is

$$\begin{aligned} M_{us}(t) = {} & A_D(t)[D - g(t)][-\sigma_{uD}(t)] + \frac{2A_S(t)}{D} \\ & \times [D - \mathrm{H}(t)] \frac{D + H(t) - 2g(t)}{2} [-\sigma_{uS}(t)] \\ & + A_B(t)[-g(t)\sigma_{yB}(t)] + \frac{A'_B(t)}{H(t)} [g(t) - D_B(t)]\{[\sigma_{uS}(t) \\ & + \sigma_{yS}(t)]D_B - H(t)\sigma_{yS}(t)\} \\ & - \frac{A_s(t)H(t)}{3D} \{[2H(t) - 3g(t)]\sigma_{uS}(t) - [H(t) - 3g(t)]\sigma_{yS}(t)\}. \end{aligned} \tag{28}$$

In the hogging condition, the ultimate moment capacity of hull is

$$\begin{aligned} M_{uh}(t) = {} & A_B(t)[D - g(t)]\sigma_{uB}(t) + \frac{2A_S(t)}{D} [D - H(t)] \frac{D + H(t) - 2g(t)}{2} \sigma_{uS}(t) \\ & + A'_B(t)[D - g(t) - D_B]\sigma'_{uB}(t) + A_D g(t)\sigma_{yD}(t) \\ & + \frac{A_s(t)H(t)}{3D} \{[2H(t) - 3g(t)]\sigma_{uS}(t) - [H(t) - 3g(t)]\sigma_{yS}(t)\}. \end{aligned} \tag{29}$$

To calculate Eq. (28) or (29), the ultimate strength of stiffened panel and unstiffened plate must be known. Paik and Lee [17] derived an empirical formula based on test results, namely

$$\sigma_u/\sigma_y = (0.995 + 0.936\lambda^2 + 0.170\beta^2 + 0.188\lambda^2\beta^2 - 0.067\lambda^4)^{-0.5}, \tag{30}$$

where λ is the column (stiffened) slenderness ratio, β is the plate slenderness ratio.

Eq. (30) is not suitable to calculate the ultimate strength of stiffened panel and unstiffened plate with crack damage. In this paper, Eqs. (1), (2), (5) and (7) are used to predict the ultimate strength of stiffened panel and unstiffened plate with crack damage.

The variance of the ultimate moment capacity of hull girder under sagging condition can be calculated as follows:

$$\begin{aligned} D_{M_{uS}(t)} = {} & \left\{ \left[D - \overline{g(t)}\right] \left[\overline{-\sigma_{uS}(t)}\right] \right\}^2 \cdot D_{A_D(t)} \\ & + \left\{ \frac{\left[D - \overline{H(t)}\right] \left[D - \overline{H(t)} - 2\overline{g(t)}\right] \overline{\sigma_{uS}(t)}}{D} \right. \\ & + \frac{\overline{H(t)}}{3D} \left\{ \left[2\overline{H(t)} - 3\overline{g(t)}\right] \overline{\sigma_{uS}(t)} \right. \\ & \left. \left. - \left[\overline{H(t)} - 3\overline{g(t)}\right] \overline{\sigma_{ys}(t)} \right\} \right\}^2 \cdot D_{A_S(t)} \\ & + \left[-\overline{g(t)\sigma_{yB}(t)}\right]^2 \cdot D_{A_B(t)} \\ & + \left\{ \frac{\left[\overline{g(t)} - D_B\right] \left[\overline{\sigma_{uS}(t)} + \overline{\sigma_{yS}(t)}\right] D_B}{H(t)} \right\}^2 \cdot D_{A'_B(t)} \end{aligned}$$

$$
\begin{aligned}
&+\left\{\frac{\overline{A_s(t)}}{D}\left(D+2\overline{H(t)}-2g(t)\right)\overline{\sigma_{us}(t)}-\frac{\overline{A'_B(t)}}{\overline{H(t)}^2}\left(\overline{g(t)}-D_B\right)\left(\overline{\sigma_{us}(t)}+\overline{\sigma_{ys}(t)}\right)D_B\right.\\
&\left.-\frac{\overline{A_s(t)}}{3D}\left[\left[4\overline{H(t)}3\overline{\mathrm{g(t)}}\right]\overline{\sigma_{us}(t)}-\left(\left[2\overline{H(t)}-3\overline{g(t)}\right]\right)\overline{\sigma_{ys}(t)}\right]\right\}^2\cdot D_{H(t)}\\
&+\left\{\overline{A_D(t)\sigma_{uD}(t)}+2\overline{A_s(t)\sigma_{sD}(t)}+\frac{\overline{A_s(t)H(t)}}{D}\left[\overline{\sigma_{ys}(t)}-\overline{\sigma_{us}(t)}\right]\right.\\
&\left.-\overline{A_B(t)\sigma_{yB}(t)}\right\}^2\cdot D_{g(t)}+\left\{\overline{A_D(t)}\left[D-\overline{g(t)}\right]\right\}^2\cdot D_{\sigma_{\mathrm{uD}}(t)}\\
&+\left\{-\frac{\overline{A_s(t)}}{D}\left[D-\overline{H(t)}\right]\frac{D+\overline{H(t)}-2\overline{g(t)}}{2}\right.\\
&\left.+\frac{\overline{A'_B(t)}}{\overline{H(t)}}\left[\overline{g(t)}-D_B\right]D_B-\frac{\overline{A_s(t)H(t)}}{3D}\left[2\overline{H(t)}-3\overline{g(t)}\right]\right\}^2\cdot D_{\sigma_{uS}(t)}\\
&+\left[\overline{A_B(t)g(t)}\right]^2\cdot D_{\sigma_{yB}(t)}\\
&+\left\{\frac{\overline{A'_B(t)}}{\overline{H(t)}}\left[\overline{g(t)}-D_B\right]\left[D_B-\overline{H(t)}\right]+\frac{\overline{A_s(t)H(t)}}{3D}\left[\overline{H(t)}-3\overline{g(t)}\right]\right\}^2\cdot D_{\sigma_{yS}(t)},
\end{aligned}
\tag{31}
$$

where

$$
\begin{aligned}
D_{C_1(t)}=&\frac{\overline{\sigma_{uD}(t)}^2\cdot D_{A_D(t)}+\overline{\sigma_{yB}(t)}^2\cdot D_{A_B(t)}+\overline{\sigma_{ys}(t)}^2\cdot D_{A'_B(t)}}{+\overline{A_D(t)}^2\cdot D_{\sigma_{uD}(t)}+\overline{A_B(t)}^2\cdot D_{\sigma_{yB}(t)}}\\
&+\frac{1}{\overline{A_S(t)}^2[\overline{\sigma_{uS}(t)}+\overline{\sigma_{yS}(t)}]^4}\left\{\left[2\overline{A_S(t)\sigma_{yS}(t)}-\overline{A_D(t)\sigma_{uD}(t)}\right.\right.\\
&\left.+\overline{A_B(t)\sigma_{yB}(t)}+\overline{A'_B(t)}\overline{\sigma_{yS}(t)}\right]^2\cdot D_{\sigma_{uS}(t)}\\
&+\left[-\overline{A'_B(t)}\overline{\sigma_{uS}(t)}-\overline{A_D(t)\sigma_{uD}(t)}-2\overline{A_S(t)\sigma_{uS}(t)}\right.\\
&\left.\left.+\overline{A_B(t)\sigma_{yB}(t)}\right]^2\cdot D_{\sigma_{yS}(t)}\right\}\\
&+\left\{\frac{\overline{A_D(t)\sigma_{uD}(t)}-\overline{A_B(t)\sigma_{yB}(t)}-\overline{A'_B(t)}\overline{\sigma_{yS}(t)}}{\overline{A_S(t)}^2[\overline{\sigma_{uS}(t)}+\overline{\sigma_{yS}(t)}]}\right\}^2\cdot D_{A_S(t)},
\end{aligned}
$$

$$D_{C_2(t)} = \left[\frac{D_B}{\overline{A_s(t)}}\right]^2 \cdot D_{A_B(t)} + \left[\frac{\overline{A'_B(t)}D_B}{\overline{A_s(t)^2}}\right]^2 \cdot D_{A_S(t)},$$

$$D_{H(t)} = \left\{\frac{1}{2}\left[D + \overline{C_1(t)}D^2\left[\overline{C_1^2(t)}D^2 + \overline{4C_2(t)}D\right]^{-\frac{1}{2}}\right]\right\} \cdot D_{c_1(t)} + \left\{\left[\overline{C_1^2(t)}D^2 + 4\overline{C_2(t)}D\right]^{\frac{1}{2}}D\right\} \cdot D_{C_2(t)},$$

$$D_{g(t)} = \left[\frac{\overline{\sigma_{yS}(t)}}{\overline{\sigma_{uS}(t)} + \overline{\sigma_{yS}(t)}}\right]^2 \cdot D_{H(t)}\left[\frac{\overline{\sigma_{uS}(t)H(t)}}{\left[\overline{\sigma_{uS}(t)} + \overline{\sigma_{yS}(t)}\right]^2}\right]^2 \cdot D_{\sigma_{yS}(t)} + \left[\frac{\overline{\sigma_{yS}(t)H(t)}}{\left[\overline{\sigma_{uS}(t)} + \overline{\sigma_{yS}(t)}\right]^2}\right]^2 \cdot D_{\sigma_{uS}(t).}$$

The variance of the ultimate moment capacity of hull girder under hogging condition can be calculated as follows:

$$\begin{aligned}
D_{M_{us}(t)} = {} & \left[\overline{g(t)\sigma_{yD}(t)}\right]^2 \cdot D_{A_D(t)} \\
& + \left\{\frac{[D - \overline{H(t)}][D + \overline{H(t)} - 2\overline{g(t)}]\overline{\sigma_{uS}(t)}}{D} + \frac{\overline{H(t)}}{3D}\{[2\overline{H(t)} - 3\overline{g(t)}]\overline{\sigma_{uS}(t)} \right. \\
& \left. -[\overline{H(t)} - 3\overline{g(t)}]\overline{\sigma_{yS}(t)}\}\right\}^2 \cdot D_{A_S(t)} + \left\{[D - g(t)]\overline{\sigma_{uB}(t)}\right\}^2 \cdot D_{A_B(t)} \\
& + \left\{[D - \overline{g(t)} - D_B]\overline{\sigma'_{uB}(t)}\right\}^2 \cdot D_{A'_B(t)} + \left\{[D - \overline{g(t)} - D_B]\overline{A'_B(t)}\right\}^2 \cdot D_{\sigma'_{uB}} \\
& + \left\{\frac{\overline{A_s(t)}}{D}\left[2\overline{g(t)} - 2\overline{H(t)}\right]\overline{\sigma_{us}(t)} - \frac{\overline{A_s(t)}}{3D}\left[4\overline{H(t} - 3\overline{\mathrm{g(t)}}\right]\overline{\sigma_{us}(t)}\right. \\
& \left. - \left(\left[2\overline{H(t)} - 3\overline{g(t)}\right]\right)\overline{\sigma_{ys}(t)}\right]^2 \cdot \mathrm{D}_{H(t)} \\
& + \left\{\overline{A_D(t)\sigma_{yD}(t)} + 2\overline{A_s(t)\sigma_{uS}(t)} + \frac{\overline{A_s(t)H(t)}}{D}\right. \\
& \left. \left[\overline{\sigma_{yS}(t)} - \overline{\sigma_{us}(t)}\right] - \overline{A'_B(t)\sigma'_{uB}(t)}\right\}^2 \cdot D_{g(t)} + \left\{\overline{A_B(t)}\left[D - \overline{g(t)}\right]\right\}^2 \cdot D_{\sigma_{\mathrm{uB}}(t)} \\
& + \left[\overline{A_D(t)g(t)}\right]^2 \cdot D_{\sigma_{yD}(t)} + \left\{\frac{\overline{A_s(t)H(t)}}{3D}\left[\overline{H(t)} - 3\overline{g(t)}\right]\right\}^2 \cdot D_{\sigma_{yS}(t)} \\
& + \left\{\frac{\overline{A_s(t)}}{D}\left[D - \overline{H(t)}\right]\left[D + \overline{H(t)} - 2\overline{g(t)}\right]\right. \\
& \left. + \frac{\overline{A_s(t)H(t)}}{3D}\left[2\overline{H(t)} - 3\overline{g(t)}\right]\right\}^2 \cdot D_{\sigma_{uS}(t)}. \qquad (32)
\end{aligned}$$

where

$$
\begin{aligned}
D_{H(t)} = D^2 \cdot & \\
& \frac{\overline{\sigma_{uB}(t)}^2 \cdot D_{A_B(t)} + \overline{\sigma'_{uB}(t)}^2 \cdot D_{A'_B(t)} + \overline{\sigma_{yD}(t)}^2 \cdot D_{A_D(t)} + \overline{A_B(t)}^2}{\{\overline{A_S(t)}[\overline{\sigma_{uS}(t)} + \overline{\sigma_{yS}(t)}]\}^2} \\
& \cdot D_{\sigma_{uB}(t)} + \overline{A'_B(t)}^2 \cdot D_{\sigma'_{uB}(t)} + \overline{A_D(t)}^2 \cdot D_{\sigma_{yD}(t)} \\
& + \frac{D^2}{\overline{A_S(t)}^2[\overline{\sigma_{uS}(t)} + \overline{\sigma_{yS}(t)}]^4} \\
& \left\{ \left[2\overline{A_S(t)\sigma_{yS}(t)} - \overline{A_B(t)\sigma_{uB}(t)} - \overline{A'_B(t)\sigma'_{uB}(t)} + \overline{A_D(t)\sigma_{yD}(t)} \right]^2 \cdot D_{\sigma_{uS}(t)} \right. \\
& \left. + \left[-\overline{A_B(t)\sigma_{uB}(t)} - \overline{A'_B(t)\sigma'_{uB}(t)} - 2\overline{A_S(t)\sigma_{uS}(t)} + \overline{A_D(t)\sigma_{yD}(t)} \right]^2 \cdot D_{\sigma_{yS}(t)} \right\} \\
& + D^2 \left\{ \frac{\overline{A_D(t)\sigma_{uD}(t)} - \overline{A_B(t)\sigma_{yB}(t)} - \overline{A'_B(t)\sigma_{yS}(t)}}{\overline{A_S(t)}^2[\overline{\sigma_{uS}(t)} + \overline{\sigma_{yS}(t)}]} \right\}^2 \cdot D_{A_S(t)}.
\end{aligned}
$$

$$
\begin{aligned}
D_{g(t)} = & \left[\frac{D\overline{\sigma_{yS}(t)}}{\overline{\sigma_{uS}(t)} + \overline{\sigma_{yS}(t)}} \right]^2 \cdot D_{H(t)} + \left[\frac{D\overline{\sigma_{uS}(t)H(t)}}{\left[\overline{\sigma_{uS}(t)} + \overline{\sigma_{yS}(t)}\right]^2} \right]^2 \cdot D_{\sigma_{yS}(t)} \\
& + \left[\frac{D\overline{\sigma_{yS}(t)H(t)}}{\left[\overline{\sigma_{uS}(t)} + \overline{\sigma_{yS}(t)}\right]^2} \right]^2 .D_{\sigma_{uS}(t)}.
\end{aligned}
$$

6. Time-variant reliability of the ship hull girder

The limit state for global hull failure is defined as

$$M_T > M_u(t), \tag{33}$$

where M_T is the total vertical bending moment acting on the hull, $M_u(t)$ is the ultimate bending moment of ship hull girder. M_T can be decomposed into two components, namely the stillwater bending moment M_s and the wave induced bending moment M_w. Since detailed load calculation is not the purpose of this study [13], we take a simplified approach to estimate the extreme total bending moment on the hull girder. The maximum stillwater bending moment is calculated from the IACS design guidance formula [18]:

$$M_s = \begin{cases} 0.015CL^2B(8.167 - C_b)(\text{KNm}) \text{ for hogging}, \\ -0.065CL^2B(C_b + 0.7)(\text{KNm}) \text{ for sagging}. \end{cases} \tag{34}$$

And the maximum wave induced bending moment M_w is calculated by

$$M_w = \begin{cases} 0.19CL^2BC_b(\text{KNm}) \text{ for hogging}, \\ -0.11CL^2B(C_b + 0.7)(\text{KNm}) \text{ for sagging}, \end{cases} \tag{35}$$

where L is the ship length, B is the ship breadth, C_b is the block coefficient, C is related to L,

$$C = \begin{cases} 0.0792L, & L < 90 \text{ m}, \\ 10.75 - [(300 - L)/100]^{1.5}, & 90 \leqslant L \leqslant 300, \\ 10.75, & 300 \text{ m} < L < 350 \text{ m}, \\ 10.75 - [(L - 300)/100]^{1.5}, & L > 350 \text{ m}. \end{cases}$$

The ratio between the mean stillwater bending moment $\overline{M_s}$ and the extreme stillwater bending moment M_S is from 0.4 to 0.6 and the coefficient of variation of M_S is from 0.3 to 0.9.

There will be a failure if Eq. (33) is fulfilled and the probability of the vertical bending moment M_T exceeding $M_u(t)$ during the period of the time $[0,T]$ is

$$P_f(T) = 1 - \exp\left[-\int_0^T v[M_u(t)]\,\mathrm{d}t\right], \tag{36}$$

where $v[M_u(t)]$ is the mean upcrossing rate of the threshold $M_u(t)$. The mean upcrossing rate is assumed to follow the Weibull distribution

$$v[M_u(t)] = v_0 \exp\left[-\left(\frac{M_u(t) - E[M_T]^{\alpha}}{\gamma}\right)\right], \tag{37}$$

where α and λ are the Weibull parameters.

Substituting:

$$R(t) = 1 - P_f(t) \tag{38}$$

in Eq. (38), the reliability after and before crack initiation can be derived as

$$R_a(t) = \exp\left(-\int_0^t v[M_u(\tau)\,\mathrm{d}\tau]\right), \quad t > t_i, \tag{39}$$

$$R_b(t) = \exp\left(-\int_0^t v[M_u(\tau)\,\mathrm{d}\tau]\right), \quad t \leqslant t_i, \tag{40}$$

where t_i is the time of the first initiation of crack propagation.

The total reliability $R(t)$ includes the reliability of the hull with cracks plus the reliability of the hull without cracks. The final expression is given by

$$R(T) = [1 - F_{T_i}(T)]R_b(T) + \int_0^T R_b(t_i)R(T - t_i)f_{T_i}(t_i)\,\mathrm{d}t_i. \tag{41}$$

The first term of this equation represents the probability that no cracks are present and that failure does not occur in time $[0,T]$. The second term

represents the probability of non-failure under the condition that the cracks are initiated.

7. Inspections and repair

It is assumed that the initial thickness of ship structures is the sum of minimum net thickness and the maximum allowable corrosion wastage:

$$t = t_{\min} + t_{\max\, w}, \tag{42}$$

where t is the initial thickness (intact thickness), $t_{\min}$ is the minimum net thickness, $t_{\max\, w}$ is maximum allowable corrosion thickness. Inspections are routinely performed for structures in service and $t_{\min}$ is the criteria that whether repair should be performed. If the plate thickness is found to be less than $t_{\min}$ at the next inspection time, in other words the corrosion wastage can be greater than $t_{\max\, w}$ at the next inspection time, the plate shall be replaced by new one with a thickness equal to its original value.

When the crack length has propagated to a limit size of detection a_d, it will be repaired. And the dimensions of element will be restored to the original state.

8. A numerical example

A double bottom tanker with a length of 168.5 m and a breath of 28 m is used to demonstrate the assessment procedure, see Fig. 7.

The midship section of the ship is divided into 159 stiffened panel elements. The dimensions of each element are shown in Table 2. The distance between transversal frames is 3925 mm.

The mean value of Young's Model E is 210000.0 MPa and the COV of E is 0.003. It is assumed that t_p, σ_Y, t_w, t_f and E obey normal distribution.

In some locations, such as the inner bottom plating and the side shells, the elements are exposed to different environments. Corrosion rate is different at each side. Then the corrosion rates should be considered, respectively. But in this paper, only the total wastage of the elements is considered. Two types of corrosion models, i.e. constant corrosion model (Model I) and a non-linear corrosion model (Model II) are used to simulate the corrosion rates. For the inner bottom plating and low sloping plating, constant corrosion model is used, and for other places, non-linear corrosion model are used. The corrosion rates are different for different elements. For one element, the corrosion rates of plating, web and flange are still different. But for one stiffener, the web and flange are usually exposed to a similar environment, and the corrosion rates are very close. So the corrosion rates of web and flange are the same, and different from the corrosion rate of the plating. Fig. 8 shows the corrosion element group number of each element and the maximum allowable wastage. And Table 3 shows the corrosion model parameters of each corrosion

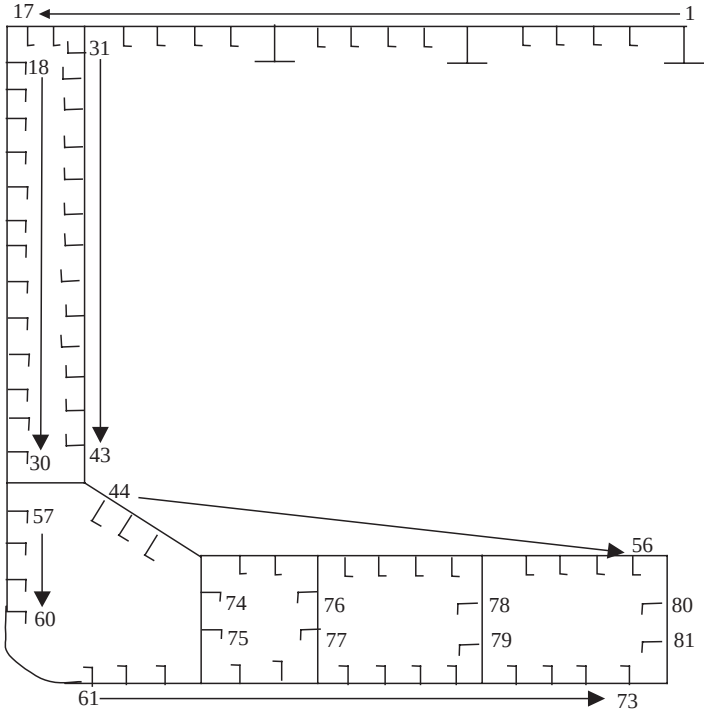

Fig. 7. Half cross section of a tanker.

element group. It must be pointed out that data in Table 3 are based on assumption rather than actual measurements.

It is assumed that all elements will be inspected every 5 years and the method of inspection is such that those elements with thicknesses can be expected to lower than the minimum net thickness $t_{\min}$ at the next inspection time are detected. New elements with a thickness equal to their original values are assumed to replace the detected plates.

Fig. 9 shows mean value of the midship section area as a function of time. And Fig. 10 shows the standard deviation of the midship section area as a function of time.

Table 4 shows the calculation results of ultimate bending moment for time equal to zero.

Figs. 11–14 show the variation of nominal initial yield bending moment, fully plastic bending moment and ultimate bending moment under the condition of repair and no repair, respectively.

For this tanker, sagging condition is the most dangerous condition. Fig. 15 shows the reliability index based on sagging ultimate bending moment. Fig. 16 shows the variation of ultimate bending moment in sagging condition.

Table 2
Dimensions and material properties of each element

Element number	Plating					Stiffener							
	b_p (mm)	t_p (mm)		σ_Y (Mpa)		h_w (mm)	tw (mm)		b_f (mm)	t_f (mm)		σ_Y (MPa)	
		Mean value	COV	Mean value	COV		Mean value	COV		Mean value	COV	Mean value	COV
16–17	800	14	0.05	235.0	0.1	200	9	0.05	90	12	0.05	353.0	0.1
12–15	800	14	0.05	235.0	0.1	300	10.5	0.05	100	15	0.05	353.0	0.1
2–5 7–10	800	12.5	0.05	235.0	0.1	350	9	0.05	90	13	0.05	353.0	0.1
18–43	750	12.5	0.05	235.0	0.1	300	10.5	0.05	120	16	0.05	235.0	0.1
44–56	750	13.5	0.05	235.0	0.1	350	10.5	0.05	120	18	0.05	235.0	0.1
61–73	750	14	0.05	235.0	0.1	350	10.5	0.05	120	16	0.05	235.0	0.1
57–60	750	12.5	0.05	235.0	0.1	350	10.5	0.05	120	16	0.05	235.0	0.1
74–81	1100	14	0.05	235.0	0.1	350	10.5	0.05	120	18	0.05	235.0	0.1
1,6,11	800	15	0.05	235.0	0.1	1050	10.5	0.05	300	15	0.05	235.0	0.1

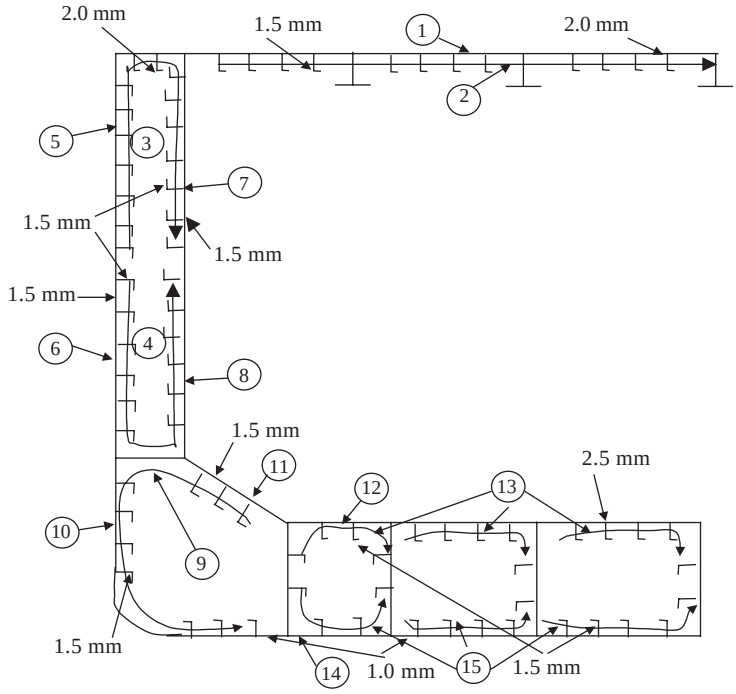

Fig. 8. Corrosion element group number and the maximums allowable corrosion thickness.

Table 3
Corrosion model parameters of each corrosion element group

Corrosion number	Corrosion model	T_{st}		d_{∞}		β		η	
		Mean value	COV	Mean value	COV	Mean value	COV	Mean value	COV
1	II	12	0.2	3.5	0.5	15	0.3	2	0.4
2	II	12	0.2	3	0.5	15	0.3	2	0.4
3	II	10	0.2	2.5	0.5	18	0.3	2	0.4
4	II	10	0.2	2.75	0.5	18	0.3	2	0.4
5	II	12	0.2	2	0.5	20	0.3	2	0.4
6	II	10	0.2	2.25	0.5	20	0.3	2	0.4
7	II	10	0.2	3	0.5	18	0.3	2	0.4
8	II	9	0.2	3	0.5	18	0.3	2	0.4
9	II	10	0.2	2	0.5	20	0.3	2	0.4
10	II	8	0.2	2.5	0.5	18	0.3	2	0.4
13	II	8	0.2	3	0.5	15	0.3	2	0.4
14	II	10	0.2	2.5	0.5	18	0.3	2	0.4
15	II	10	0.2	2.25	0.5	18	0.3	2	0.4
11	I	0.13 mm/year					COV0.5		
12	I	0.14 mm/year					COV0.5		

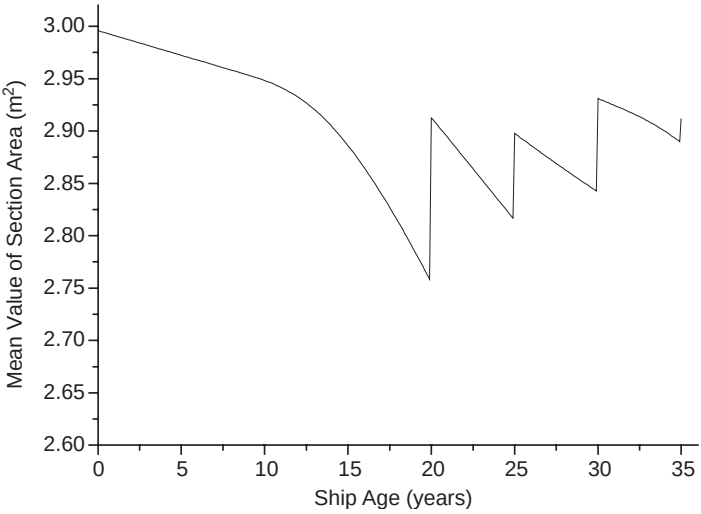

Fig. 9. Mean value of the midship section area as a function of time.

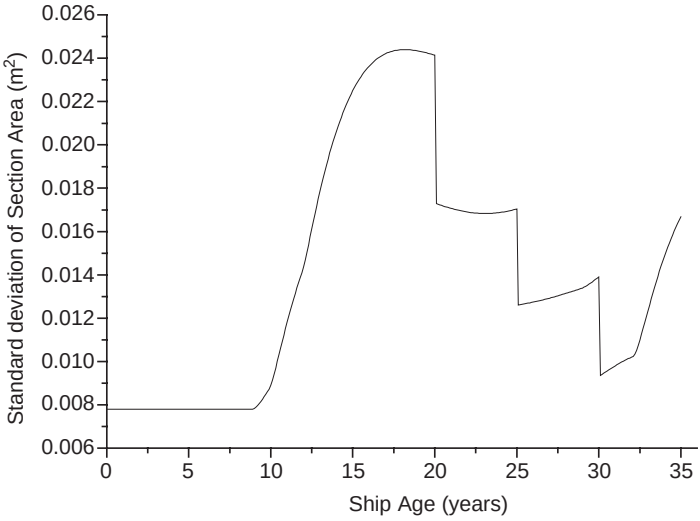

Fig. 10. Standard deviation of the midship section area as a function of time.

Table 4
Bending moment for $T = 0$

Initial yield bending moment M_{Y0}	Fully plastic bending moment M_{p0}	Ultimate bending moment	
		Sagging M_{US0}	Hogging M_{UH0}
3.82×10^9 Nm	5.31×10^9 Nm	4.03×10^9 Nm	4.69×10^9 Nm

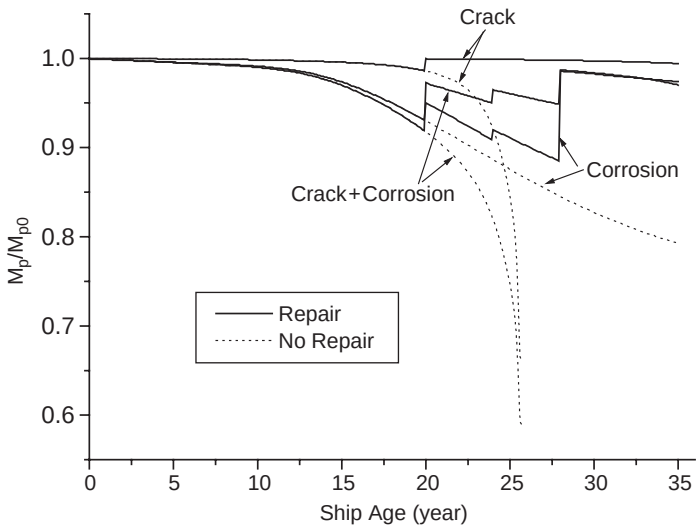

Fig. 11. Mean value variation of fully plastic bending moment with time.

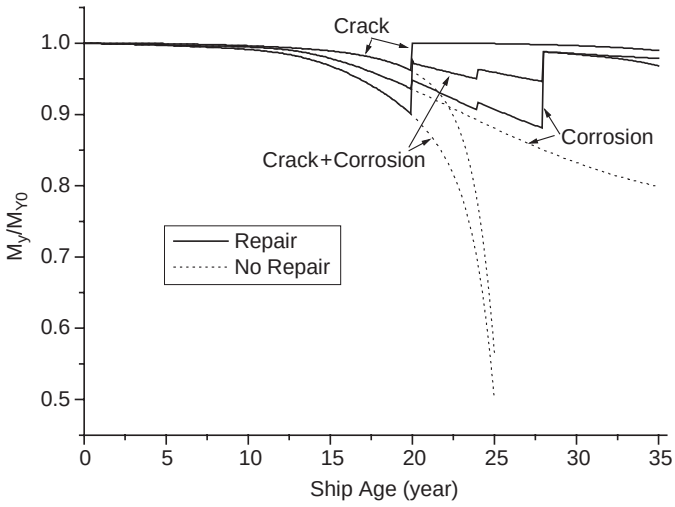

Fig. 12. Mean value variation of initial yielding bending moment with time.

If one assumes that the ultimate bending moment of hull girder obey normal distribution in sagging condition, Fig. 17 shows the probability density at each repair year for the sagging condition. In Fig. 17, the solid line curves represent the probability density before repair and the dot line curves represent he probability density after repair.

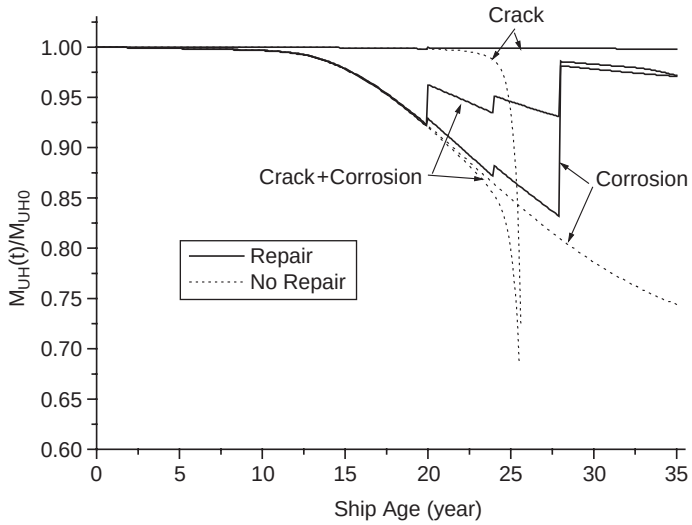

Fig. 13. Mean value variation of ultimate bending moment with time under hogging condition.

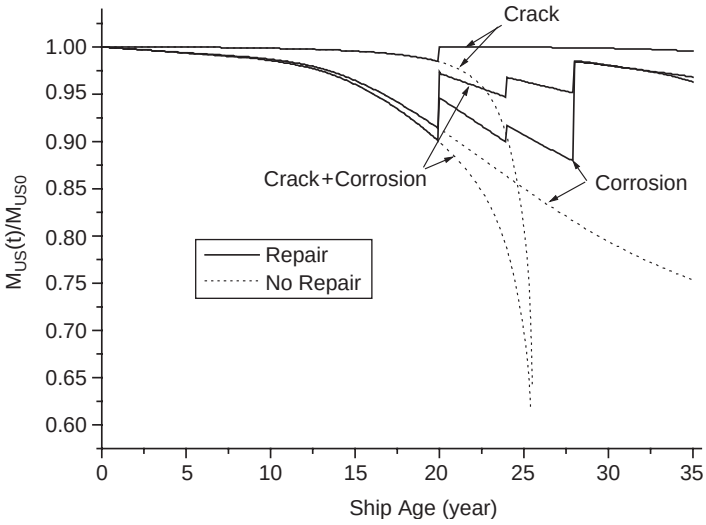

Fig. 14. Mean value variation of ultimate bending moment with time under sagging condition.

9. Discussion about $t_{\max w}$

The parameter $t_{\max w}$ is very important, which not only determines the repair time but also the repair cost to certain extent. The allowable corrosion thickness $t_{\max w}$ can be determined by the following method. The residual ultimate bending moment

Fig. 15. The reliability index based on sagging ultimate bending moment.

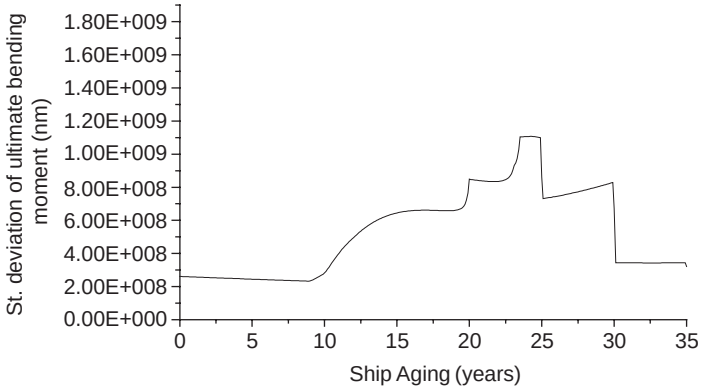

Fig. 16. Standard deviation of ultimate bending moment.

of hull girder has a minimum allowable service value M_{Ua} to resist external bending moment. And the residual ultimate strength $\sigma_u(t)$ for each element also has a minimum allowable residual ultimate strength σ_{ua} to resist the local loads. When the ultimate bending moment of hull girder has degraded to M_{Ua}, or the residual ultimate strength for each element has degraded to σ_{ua}, the ship hull should be repaired. The degree of repair depends on (1) how much the strength should be improved, (2) how long the repaired ship can be used before the ultimate strength degrade to M_{Ua} or the local strength degrade to σ_{ua} again, and (3) the repair cost. Here one can simply assume that the repair area A_r can determine the repair cost. So the repair goal is to repair a small area A_r and to obtain a longer period T_r from repair moment to the moment that the ultimate bending moment degrades to M_{Ua} again. And then T_r/A_r is one of the important repair indicators. Another repair

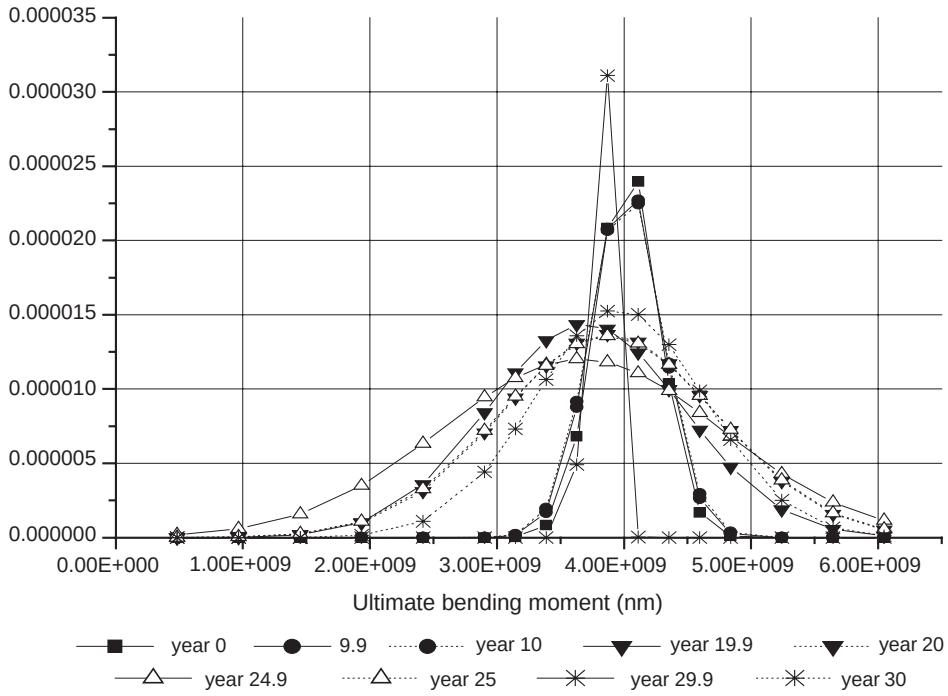

Fig. 17. The probability density at each repair year for the sagging condition.

indicator is the minimum allowable local residual ultimate strength σ_{ua}. The local ultimate strength should not reduce to σ_{ua} before the next repair time. Let us assume that M_{Ua} is 90% of M_{US0} and the ship can be used more than 6 years after repair. The allowable residual local ultimate strength of each element σ_{ua} has simply assumed as 80% of initial ultimate strength σ_{ua0}. The ship hull cross section is simply divided into five repair zones; those are deck, upper side shell, lower side shell, inner bottom and outer bottom. In fact, for each of the five repair zones, the repair time is different for each element. If we divide the ship hull cross section into more repair zones, we can obtain more accurate repair time.

Fig. 18 shows the variation of degradation of compressive and tensile residual ultimate strength for different parts of the elements with time. In Fig. 18, the residual ultimate strength is nominal residual ultimate strength, which equals to $\sigma_u(t)/\sigma_{ua0}$.

Table 5 shows the repair time of each repair zone and the corrosion thicknesses of plating and stiffener at the repair time. The repair time is only according to the local structure repair indicator σ_{ua}. The repair rule is that the element should be repair when the compressive or tensile ultimate strength reduce to 80% of its initial value σ_{u0}.

The dimension of each element must be larger than a certain value to resist not only the local load but also the external bending moment. Another repair rule that

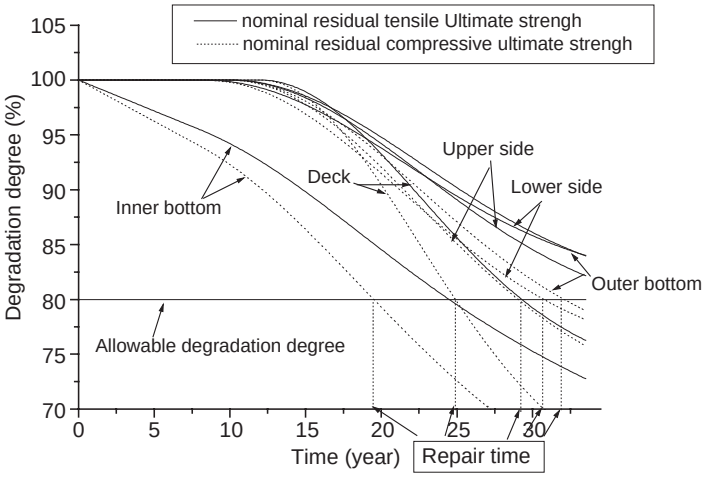

Fig. 18. Variation of residual compressive and tensile ultimate strength for different element.

Table 5
Mininmum allowable corrosion thickness to deal with local loads

Element place	Repair time (years)	Corrosion thickness for σ_{ua} reducing to 80% of σ_{ua0} (mm)		Loading type
		Plating	Stiffener	
Deck	25	1.8	1.6	Compression
Upper side	30	2.0	1.7	Compression
Lower side	30.5	2.0	1.3	Compression
Inner bottom	19.5	2.5	1.3	Compression
Outer bottom	32.0	1.9	1.7	Compression

the ship hull girder ultimate bending moment $M_U(t)$ is greater than M_{Ua} must be satisfied. For this tanker, when the ultimate bending moment reduces to minimum allowable service value M_{Ua}, the ship age is 22 years. To improve the ultimate bending moment at the age of 22 years, one or more of the five repair zones should be repaired. Fig. 19 shows the variation of the ultimate bending moment by repairing different repair zone, respectively, at the age of 22 years.

From Fig. 19, one can find that the inner bottom should be repaired before 22 years due to the insufficiency of local strength. So the repair time for the inner bottom is 19.5 years. And the maximum allowable corrosion thicknesses for inner bottom are 2.5 mm for plating and 1.3 mm for stiffener, see Table 5.

Table 6 is the comparison of repairing different repair zones at the age of 22 years.

In Table 6, the repair priority is determined by the following rules that (1) the period T_r, which is the time from repair moment 22 years to the moment that the ultimate bending moment degrades to M_{Ua} again, must be greater than 6 years, (2)

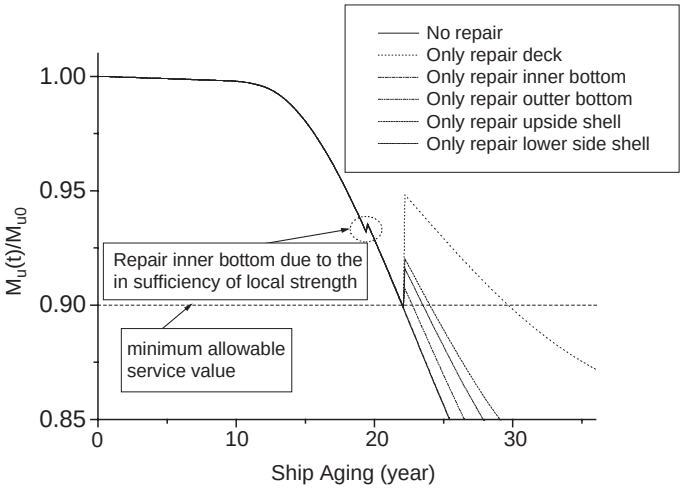

Fig. 19. The variance of ultimate bending moment by repairing different repair zones at the first repair time due to the insufficiency of ultimate bending moment.

Table 6
Comparison of repairing different repair zone that the age of 22 years

Repair zone	T_r(year)	A_r (m^2)	T_r/A_r	Corrosion thickness		Priority
				Plate (mm)	Stiffener (mm)	
Deck	6.6	0.4389	15.03759	1.7	1.4	1
Inner bottom	0.8	0.4855	1.647786	2.0	1.40	5
Outer bottom	1.0	0.5393	1.854256	0.8	0.7	4
Upside shell	2.0	0.3812	5.24659	0.7	0.6	2
Lower side shell	1.6	0.6149	2.602049	0.8	0.7	3

the value of T_r/A_r is the largest one. From Table 6, one can find that the deck should be repaired first. If only the deck is repaired, the ship can be used more than 6 years (7.6 years). And then, the maximum allowable corrosion thickness for deck can be found at the year of 22 year. The maximum allowable corrosion thicknesses for deck are 1.7 mm for plating and 1.4 mm for stiffener.

If only the deck is repaired, the ultimate bending moment will reduce to M_{US0} again at the age of 29.5 years. The same method can be applied to determine the repair priority at the age of 29.5 years, see Table 7. From Table 7, one can find that the upside shell should be repaired first at 29.5 years. If only repair the upside shell at the age of 29.5 years, the value of T_r is still more than 6 years (6.5 years). And then, the maximum allowable corrosion thicknesses for the upside shell can be found, that is 2.0 mm for plating and 1.7 mm for stiffener.

By using the same method, the maximum allowable corrosion thicknesses for lower side shell and outer bottom can be found. The outer bottom and lower side

Table 7
Comparison of repairing different repair zone at the age of 29.5 years

Repair zone	T_r(year)	A_r(m^2)	T_r/A_r	Corrosion thickness		Priority
				Plate (mm)	Stiffener (mm)	
Deck	0	0.4389	0	0	1.4	5
Inner bottom	0.3	0.4855	0.62	0.1	0	4
Outer bottom	4.1	0.5393	7.6	0.8	0.9	3
Upside shell	6.5	0.3812	17.05	2.0	1.7	1
Lower side shell	9.2	0.6149	14.96	1.1	0.7	2

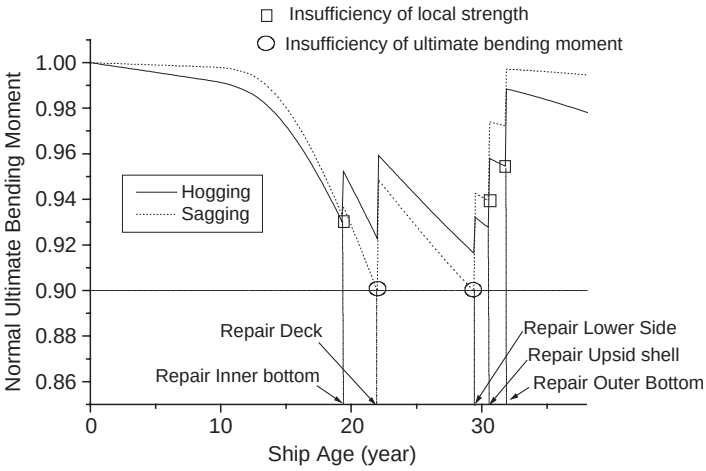

Fig. 20. Repair time and repair reason for diferent repair zone.

Table 8
Finial results about maximum allowable corrosion thicknesses

$t_{\max\ w}$	Deck	Inner bottom	Outer bottom	Upside shell	Lower side shell
Plate	1.35	3.26	1.78	1.42	2.1
Stiffener	1.1	2.71	1.98	2.1	2.3

shell should be repaired, respectively, at 30.5 and 32 years. The repair reason is the insufficiency of the local strength.

The final results are shown in Fig. 20 and Table 8.

10. Summary and conclusions

In this paper, a methodology to assess the time-variant ultimate strength of ship hull girder under the degradations of corrosion and fatigue is proposed. In this

methodology, the influences of corrosion and fatigue on the ultimate strength are considered.

To calculate the ultimate bending moment of ship hull girder, the influence of crack on the residual ultimate strength of the unstiffened plate and the stiffened panel has been discussed. A simplified FE method is used to calculate the residual ultimate tensile and compressive strength of cracked unstiffened plates and stiffened panels. Based on the FE analysis results, some empirical formulae are obtained, Eqs. (1)–(3). Those formulae are also valid to calculate the ultimate strength of intact unstiffened plates and stiffened panels.

Linear and non-linear corrosion models are used to predict the corrosion wastage of plating and stiffener. For inner bottom plating and low sloping plating, the main reason for wastage are uncoating and friction. Linear corrosion model is used to calculate the wastage to those plates. And for other places, a four-parameter non-linear model is used to simulate the corrosion rate. The corrosion rates are different for the plating and stiffener. The corrosion rate depends on the location of the element. And the allowable wastage thicknesses are different for each element.

In this paper, a minimums net thickness rule is used to determine repair policies. A procedure to determine the maximum allowable corrosion thickness is demostrated. The maximum allowable corrosion thickness is according to the rules that (1) how much the strength should be improved, (2) how long the repaired ship can be used before the ulitmate strength degrade to M_{Ua} or the local strength degrade toσ_{ua} again, and (3) the repair cost.

The procedures developed in the present study should be useful for assessing ultimate strength reliability of aging hulls taking into account the degradation effects of corrosion and fatigue crack. The described methodology is applied to assess a double bottom tanker. The calculation results indicate influences of the fatigue crack, corrosion and repair on the ultimate strength reliability of the ship hull girder.

Reference

[1] Yao T. Hull girder strength. Mar Struct 2003;16:1–13.
[2] Guedes Soares C, Garbatov Y. Fatigue reliability of the ship hull girder. Mar Struct 1996;9:495–516.
[3] Guedes Soares C, Garbatov Y. Reliability of maintained ship hull girders subjected to corrosion and fatigue. Struct Safety 1998;20:201–19.
[4] Guedes Soares C, Garbatov Y. Reliability of corrosion protected and maintained ship hulls subjected to corrosion and fatigue. J Ship Res 1998;43(2):65–78.
[5] Guedes Soares C, Garbatov Y. Reliability of maintained ship hulls subjected to corrosion and fatigue under combined loading. J Constr Steel Res 1999;52:93–115.
[6] Paik JK, Thayamballi AK, Kim SK, Yang SH. Ship hull ultimate strength reliability considering corrosion. J Ship Res 1998;42(22):154–65.
[7] Paul HW, James F, Anil T. Reliability with respect to ultimate strength of a corroding ship hull. Mar Struct 1997;10:501–18.
[8] Hu Y, Cui WC. A simplified analytical method to predict the ultimate strength of unstiffened plates under combined loading including edge shear. J Ship Mech 2003;7(6):60–74.
[9] Cui WC, Wang YJ, Pedersen PT. Strength of ship plates under combined loading. Mar Struct 2002;15:75–97.

[10] Paik JK, Thayamballi AK. Ultimate strength of aging ships. J Eng Maritime Environ 2002; 216(M1):57–77.
[11] Paik JK, Kim SK, Lee SK. Probabilistic corrosion rate estimation model for longitudinal strength members of bulk carriers. Ocean Eng 1998;25:837–60.
[12] Qin SP, Cui WC. Effect of corrosion models on the time-variant reliability of steel plated elements. Mar Struct 2003;16:15–34.
[13] Baarholm GS, Moan T. Estimation of nonlinear long-term extremes of hull girder loads in ships. Mar Struct 2000;13:495–516.
[14] Vasta J. Lessons learned from full-scale structural tests, Trans SNAME 1958;66:165–243.
[15] Caldwell JB. Ultimate longitudinal strength, Trans RINA 1965;107:411–430.
[16] Paik JK, Mansour AE. A simple formulation for predicting the ultimate strength of ships. J Mar Sci Technol 1995;1:52–62.
[17] Paik JK, Lee JM. An empirical formulation for predicting ultimate compressive strength of plates and stiffened plates. Trans Soc Naval Archit Korea 1996;33(3):8–21 [in Korean].
[18] Nitta A, Aral H, Magaino A. Basis of IACS unified longitudinal strength standard. Mar Struct 1992;5(1):1–21.